RICE UNIVERSITY

Comparison of Laser-Produced Plasma Target Materials for Pumping the 109 nm Xe^{2+} Auger Laser

by

Tasshi Dennis

A THESIS SUBMITTED
IN PARTIAL FULFILLMENT OF THE
REQUIREMENTS FOR THE DEGREE

Master of Science

APPROVED, THESIS COMMITTEE:

James F. Young, Chairman
Professor of Electrical and Computer Engineering

Frank K. Tittel
Professor of Electrical and Computer Engineering

William L. Wilson
Professor of Electrical and Computer Engineering

Houston, Texas

May, 1995

Comparison of Laser-Produced Plasma Target Materials for Pumping the 109 nm Xe^{2+} Auger Laser

Tasshi Dennis

Abstract

Short wavelength lasers have many potential applications in scientific and engineering fields. The goal of this research was to improve the output energy of the Xe^{2+} 109 nm laser. We compared cadmium, copper, gold, and zinc targets to stainless steel for laser-produced plasma pumping the Xe laser. A unique target geometry allowed us to measure the laser output using two materials under identical conditions. Small signal gain coefficients and maximum output powers are presented for each material relative to stainless steel; we observed a $\sim$ 20% improvement in the gain coefficient and a $\sim$ 112% improvement in total energy using a cadmium target. This increase probably results from an improved overlap of the laser-produced plasma emission spectrum with the Xe inner shell $4d$ photoionization cross section, although published data to support this hypothesis are scarce and inconsistent.

Acknowledgments

I would like to thank the many people that have made my master's work a fruitful and enjoyable experience. First, I would like to express my gratitude toward my thesis advisor Jim Young for conceiving my master's project and for providing continued guidance during the whole of my graduate work. I am especially gratiful for the thoughtful guidance he provided during the early stages of my master's work, making it a smooth and concise process.

I would also like to thank Dr. Frank Tittel and Dr. Bill Wilson for their participation on my thesis committee, spending precious time at the end of a semester to read and evaluate my thesis work.

For their experimental work, I thank Jun Wu, Dr. Csaba Toth, and Dr. Matt Duiker. All three must be thanked for their involvement with data collection and their help operating and maintaining a tempermental experimental apparatus. I am particularly gratiful to Matt for providing a critical eye both in and out of the lab, and for his encouragement to attempt new challenges.

Special thanks are extended to my parents, who have supported all my endeavors to this date. I am especially thankful for their support during those times of particular challenge.

This research was supported by the Air Force Office for Scientific Research, and the National Science Foundation.

Table of Contents

List of Figures

List of Tables

Chapter 1

Introduction

Vacuum ultraviolet (VUV) lasers have proven to be useful tools for applications in photochemistry, photolithography, imaging, medicine, and materials science. The 109 nm Xe^{2+} Auger laser is a promising practical source of VUV radiation because of its unique combination of high gain, efficiency, benign physical properties, and short wavelength. For its intended application of imaging and holography, the Xe laser is required to produce sufficient output energy to expose a holographic or imaging medium. Since improvements in performance without added complexity to the laser would increase its practicality for real application, we choose to examine various target materials for pumping the Xe laser.

Laser-produced plasmas have proven to be convenient pumping sources for VUV lasers [1, 2, 3, 4, 5, 6]. In these experiments, a short pulse length laser is focused to high intensity on a metal target, forming and heating a high density, highly ionized plasma. Typically, the focal region is a line with a power density of 10^{11} to $10^{13}\,\mathrm{Wcm^{-2}}$. The hot plasma radiates incoherent soft x-rays into the surrounding gas, and creates

a population inversion either through direct photoionization or via collisions with energetic electrons produced by photoionization. The practicality of this pumping method, and of the VUV lasers, depends critically on the conversion efficiency of laser light into soft x-ray radiation with the required spectrum, since higher efficiency reduces the size and cost of the required pump laser system. VUV lasers are single-pass amplifiers seeded by spontaneous emission, with much of the gain length operating in the small-signal, exponential gain regime; thus, small improvements in pumping efficiency can yield large improvements in output power and overall efficiency.

As shown in Fig. 1.1, a Xe laser energy level diagram, pumping begins with the photoionization of an inner shell $4d$ electron from neutral Xe. The threshold for Xe $4d$ photoionization is 68 eV, corresponding to the energy range of soft x-ray emission. The $4d$ photoionization has a peak cross section of 1.8×10^{-17} cm^2 at 100 eV and a full width at half maximum of about 40 eV as shown in Fig. 1.2 from Holland, et al. [7]. In this range, the photoionization cross section for $4d$ inner electrons is about ten times larger than that for the outer $5s$, $5p$ electrons. The resulting ion, Xe II $4d^9 5s^2 5p^6$, rapidly undergoes Auger decay to form various states of Xe III. The decay process has a 5% yield into both Xe III $4d^{10} 5s^0 5p^6$ and Xe III $4d^{10} 5s^1 5p^5$, forming the upper and lower laser levels, respectively. A population inversion is created by the 3 to 1

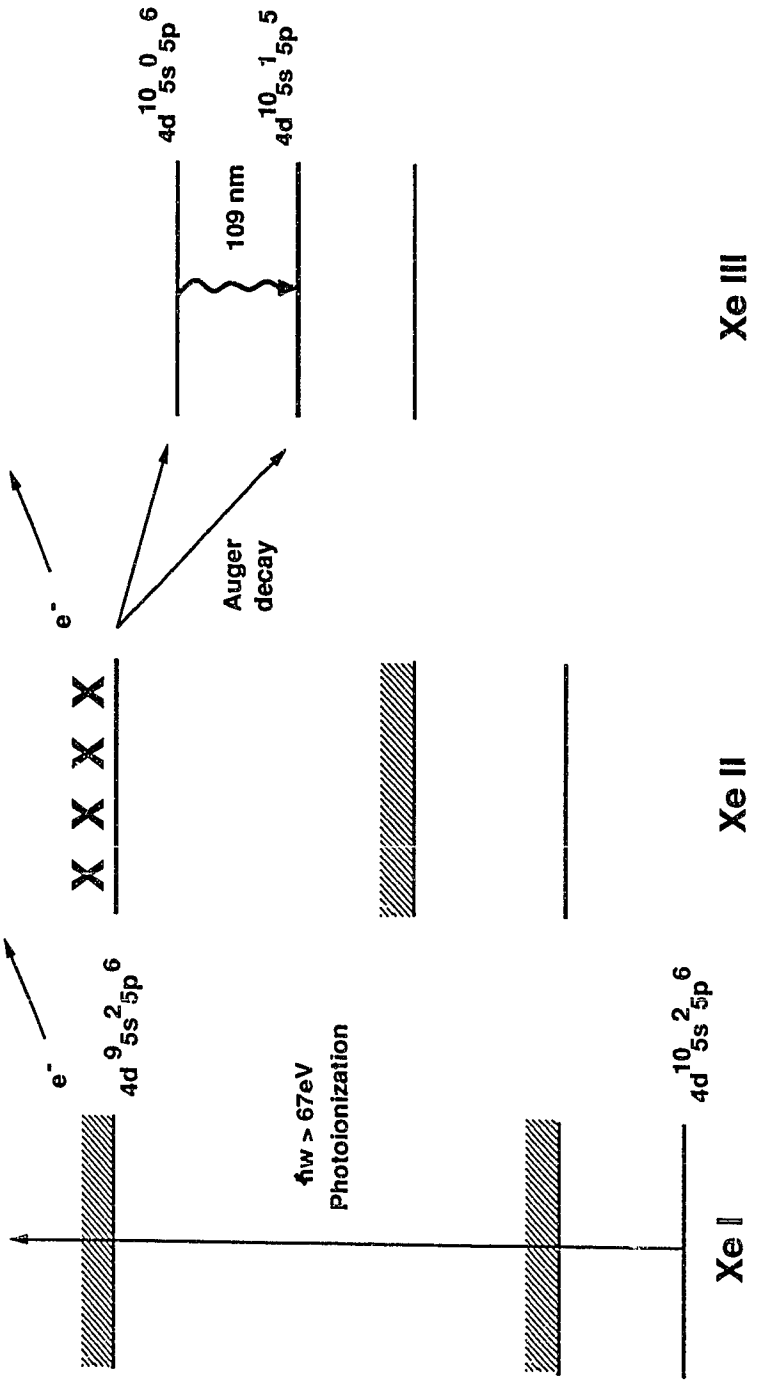

Figure 1.1: The Xe^{2+} laser energy level and transition diagram.

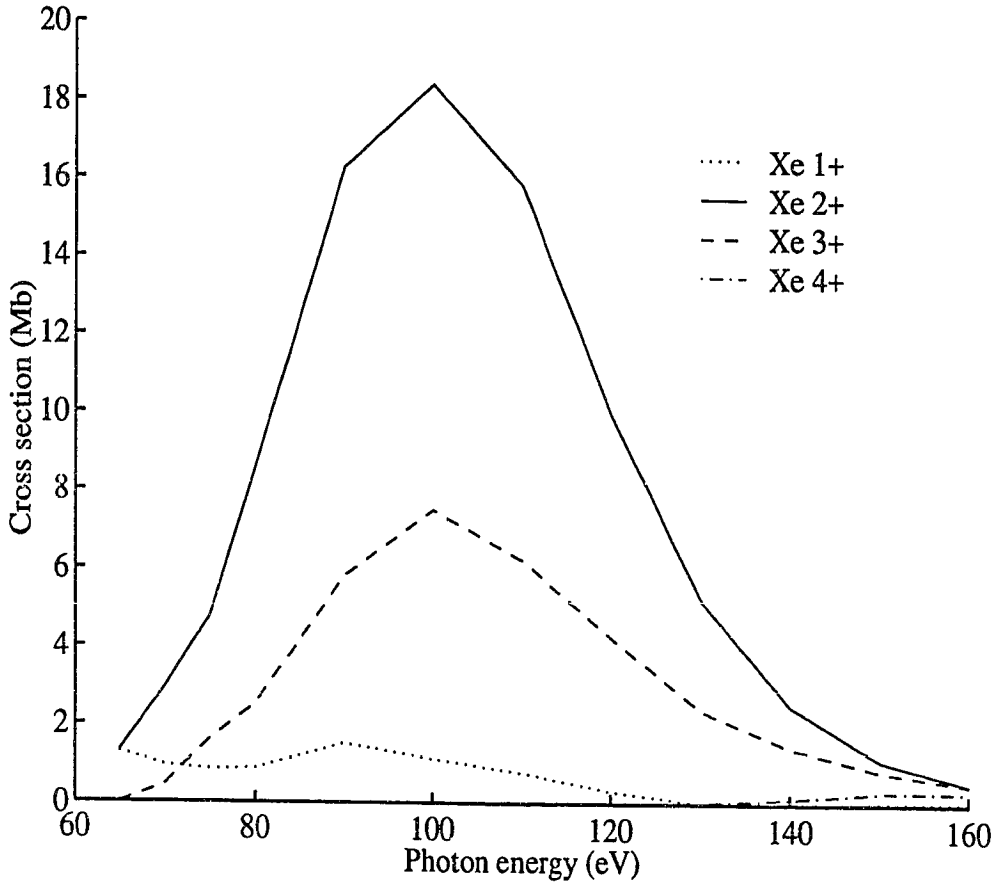

Figure 1.2: Partial photoionization cross sections for xenon. Plot reproduced from the data of Holland, et al.

degeneracy of the lower energy state relative to the upper. A spontaneous transition between these levels results in emission at 109 nm.

Maximization of the seemingly simple pumping process requires a detailed knowledge of the laser-produced plasma emission process. This, however, is not a trivial requirement. Many experiments, theories, and computer models have been generated to measure and predict the plasma spectrum under various pump laser conditions for various target materials [8, 9, 10]. A number of these studies have focused on pumping conditions and plasma energy regimes for laser fusion experiments, with conditions far above those used for pumping the Xe laser. Laser-produced plasmas are commonly modeled as black body sources with an effective temperature. However, this description is useful only in a qualitative sense, owing to the distinct spectral features of real plasma spectrums. Probably the best theory to date describes the heating of plasma electrons by inverse Bremsstrahlung, or collisional absorption. Penetration of the laser light into the target material creates a population of free electrons. As the electrons oscillate in the optical field, they may experience dephasing collisions, resulting in the permanent transfer of energy from the field to the electrons. Subsequent collisions of the hot electrons with ions of the target material result in the production of more electrons and the elevation of the ions to higher stages of ionization. Relaxation

of the hot ions to lower levels produces the plasma radiation spectrum. Thus, in this respect, soft x-ray intensity and spectra are strongly dependent on the ability of the irradiated target material to produce a large electron density and to ionize to higher energy levels. This leads to the useful, yet simplistic, view that materials of high atomic number, composed of many electrons and ionization levels, should have broader and more intense plasma spectra.

Several target materials have been used previously for the Xe^{2+} laser. The first observations of gain in the Xe Auger system were reported in 1986 using a tantalum target [1]. G. Yin, et al., also used tantalum in their optimization studies [11]. In 1987, Sher, et al., used an electroplated gold target and a new pump geometry, and reported the first saturated Xe^{2+} laser output [12]. In later experiments, this group also reported results using a stainless steel target [13]. Our initial Xe^{2+} laser system also used a stainless steel target, primarily because of its simplicity [14]. Since the pump laser energy, pulse length, and focused intensity on target vary considerably among these experiments, it is difficult to isolate the effect of the target material on Xe^{2+} laser performance. Recently, however, the performance of a self-healing, Hg-coated gold target has been compared to that of a plain gold target under comparable conditions; the two had similar performance [15].

We conducted the first experiments that quantitatively compare cadmium, copper, gold, zinc, and stainless steel plasma targets for pumping the 109 nm Xe^{2+} Auger laser under identical experimental conditions. Use of a cadmium target more than doubles the laser output energy. This increase probably results from an improved overlap of the laser-produced plasma emission spectrum and the Xe inner shell $4d$ photoionization cross section.

Chapter 2

Experiment

The target geometry and laser configuration of our system allowed for a near-simultaneous comparison of two target materials. The design and operation of a practical Xe Auger laser has been described previously [14]. As shown in Fig. 2.1, the pumping system begins with a Coherent Antares 76-s Nd:YAG CW modelocked oscillator, providing a 76 MHz train of $\sim$ 100 psec or $\sim$ 200 psec [16] long pulses at 1064 nm. The first target experiment, comparing gold and stainless steel, utilized the $\sim$ 200 psec long pulses. For subsequent experiments, however, improvements to the pump system allowed the shorter $\sim$ 100 psec pulses to be used without damage to the optical components. A Continuum RGA–69 pulsed regenerative amplifier and a single pass 9 mm Nd:YAG amplifier were used to amplify selected pulses to an energy of about 260 mJ. Since the output beam of the regenerative amplifier was apertured and not an eigenmode of free space propagation, relay imaging optics [17] were used throughout to maintain fringe-free beam patterns and to expand the beam to a diameter of 2.5 cm. The pump system was capable of amplifying pulses at a rate of 6 Hz. Before each

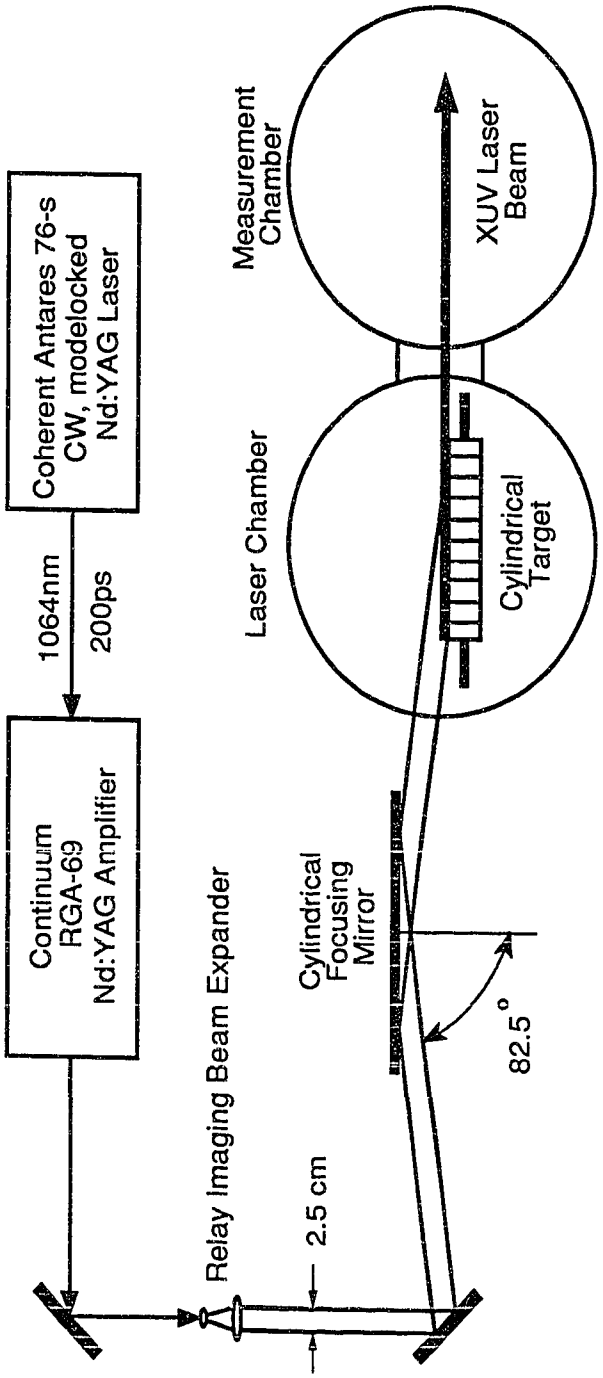

Figure 2.1: Pumping system for the 109 nm Xe^{2+} Auger laser.

experiment, the pulse duration and beam profile of the pump laser were optimized, and the pulse energy was adjusted to the 260 mJ value. The pump beam was focused to a $\sim 75\,\mu$m wide by 20 cm long line on the grooved target using a cylindrical mirror at an 83 deg angle of incidence, resulting in a power density of about $10^{11}\,\mathrm{Wcm^{-2}}$. This glancing geometry results in a quasi-traveling wave propagation of the pump beam.

The basic plasma target was a machined stainless steel rod 3.8 cm in diameter and 20 cm long, threaded at ~ 30 grooves per centimeter. The sample material was electroplated over half the circumference of the basic target, while the other half was left unplated to provide a reference signal from stainless steel. Targets were prepared using cadmium, copper, gold, and zinc. Plating was done at local industral plating companies, with no guarantees of material purity. However, we do not expect purity variations of a few percent to have significant impact on target performance. By using local plating services, the cost of Xe laser operation was kept to a minimum. The plating companies estimated the thickness to be $12\,\mu$m for the gold, and about $75\,\mu$m for the others. While an unplated target requires surface cleaning with acetone to remove machining lubricants, this was unnecessary for plated targets, which were cleaned during the plating process. As shown in Fig. 2.2 rotation of the rod during

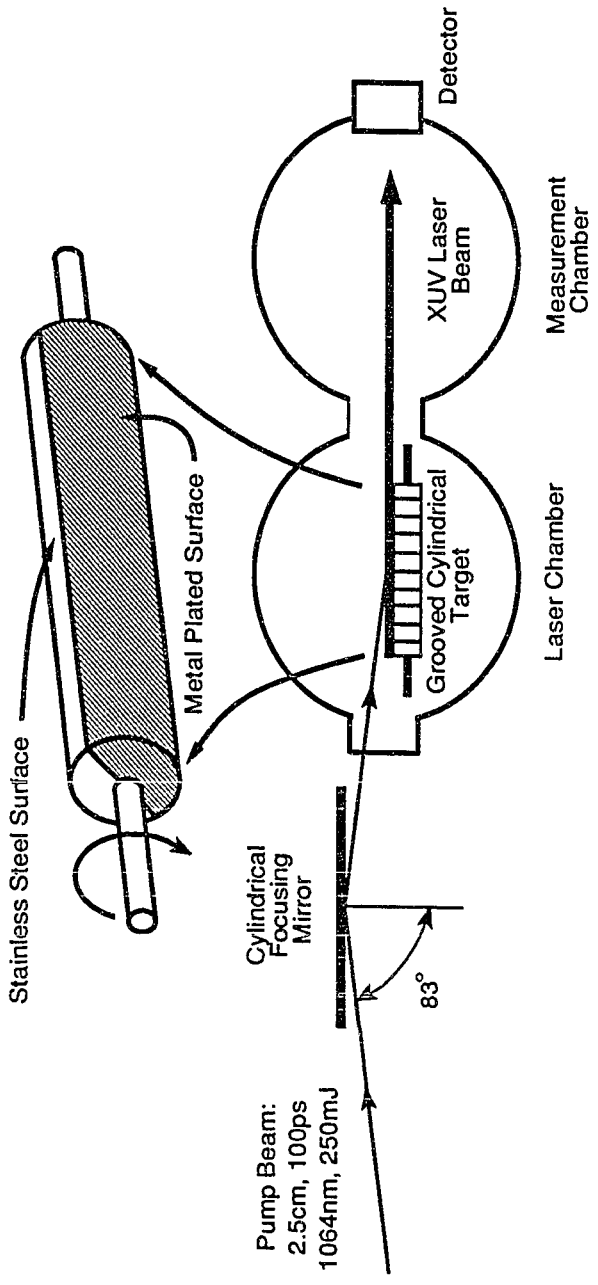

Figure 2.2: Target geometry for the 109 nm Xe^{2+} Auger laser.

laser operation exposed alternating sections of stainless steel and the plated sample material to the pump pulses.

The target rod was housed in a vacuum cell containing $\sim$ 15 Torr of Xe gas, a pressure found to be optimum in previous studies [14]. The output intensity of the forward propagating 109 nm beam was measured with an aluminum oxide cathode photodiode and oscilloscope. The length of the target pumped was varied using a moveable knife edge placed in the pump beam outside the target chamber. For each pumped length, the laser output energy was recorded for both the stainless steel and the plated metal regions as the target rotated. In this manner, data for the sample material and stainless steel were collected in alternating measurements while maintaining near-identical pumping conditions.

Chapter 3

Results

Figure 3.1 shows a semilogarythmic plot of the laser output as a function of plasma length using a stainless steel target with a gold plated region. Measurable output energy was obtained for a pumped length of only $\sim 7\,\mathrm{cm}$ from the gold target region, whereas the stainless steel region required nearly 9 cm. The first three points of each curve were fit to a straight line to estimate the small signal gain coefficients: approximately $1.6\,\mathrm{cm}^{-1}$ for gold, and $1.3\,\mathrm{cm}^{-1}$ for stainless steel. For both materials, the output energy dependence on pumped length deviated strongly from exponential for target lengths greater than 13 cm, indicating saturated behavior. Plots for the gold-stainless steel target show a functional behavior similar to previous Xe^{2+} laser studies with gold targets.

The same procedure was repeated for stainless steel targets plated with cadmium and zinc. Plots of these results are shown in Figs. 3.2 and 3.3. Again, we observed exponential behavior for at least the first three data points of all the curves. The small signal gain coefficient for cadmium was found to be approximately $1.50\,\mathrm{cm}^{-1}$

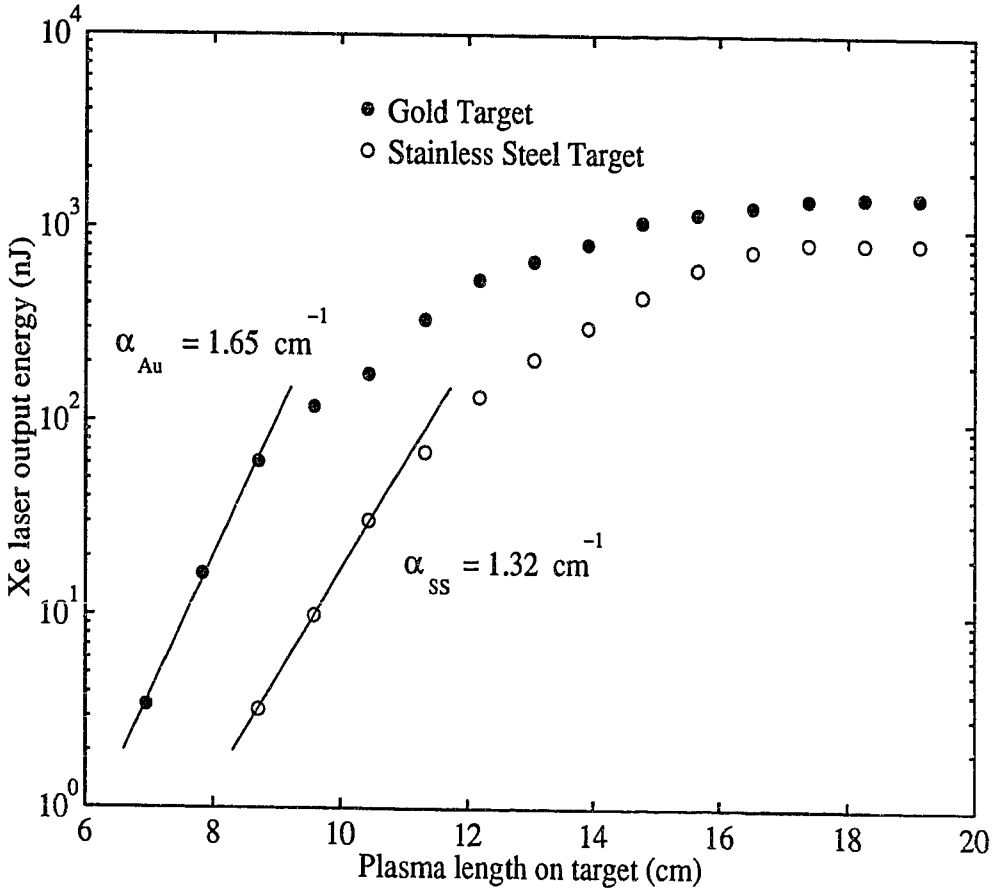

Figure 3.1: Xe laser output energy vs. plasma length for the gold-stainless steel target.

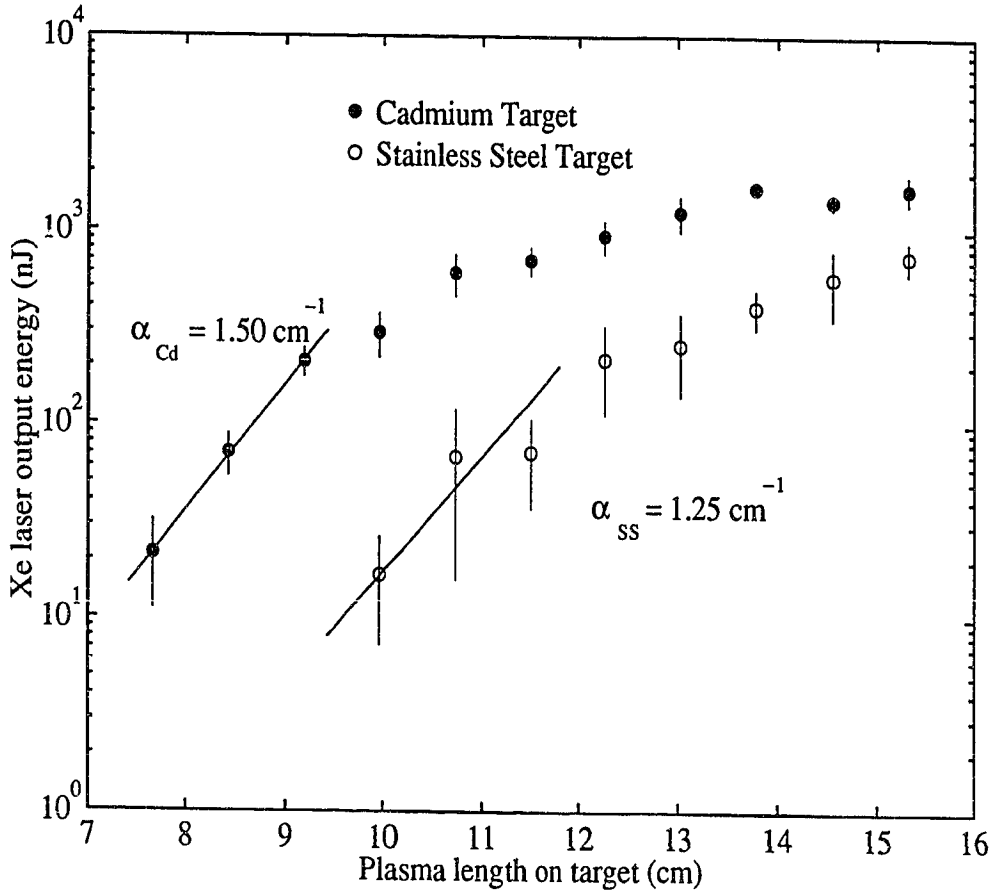

Figure 3.2: Xe laser output energy vs. plasma length for the cadmium-stainless steel target.

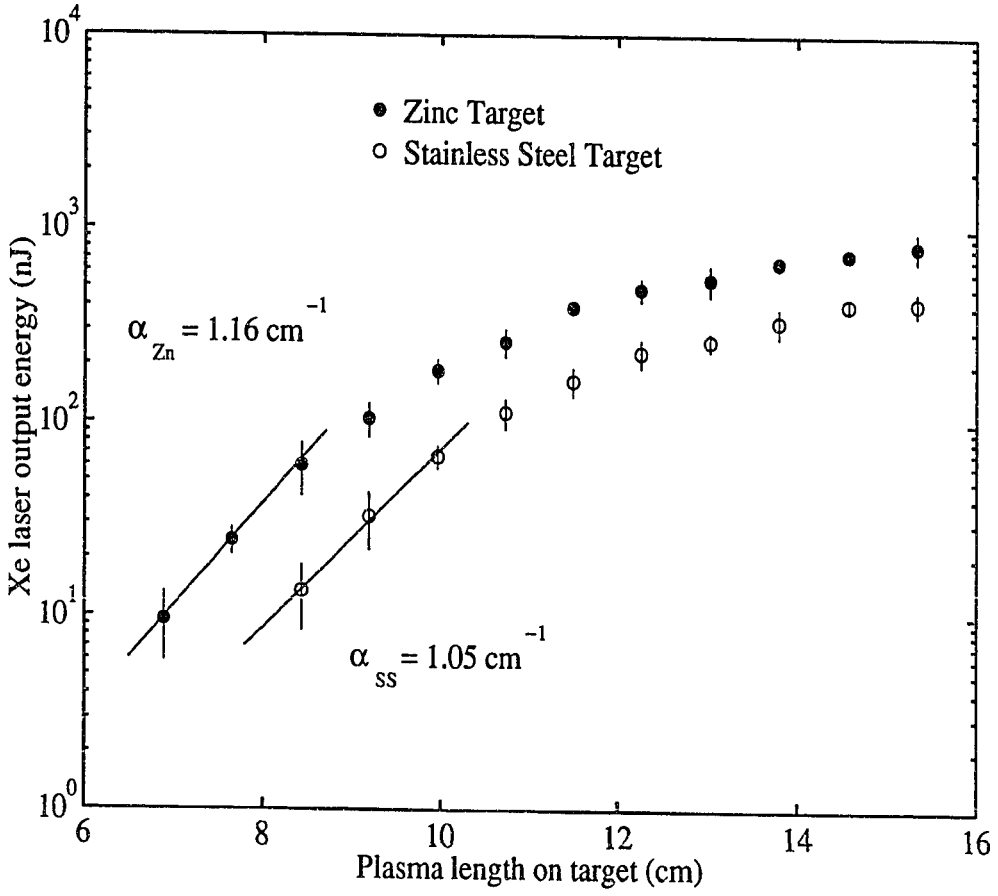

Figure 3.3: Xe laser output energy vs. plasma length for the zinc-stainless steel target.

as compared to 1.25 cm^{-1} for the bare stainless steel. Zinc had a gain of 1.16 cm^{-1} as compared to 1.05 cm^{-1} for stainless steel. This is an improvement in small signal gain of $\sim$ 20% for cadmium and $\sim$ 11% for zinc. For full target illumination, cadmium displayed a $\sim$ 112% improvement in Xe laser output energy, while zinc displayed $\sim$ 100%. This data, and that for the copper target to be discussed later, are summarized in Table 3.1.

Material	Total output improvement	Small signal gain improvement
Cadmium	112%	20%
Zinc	100%	11%
Gold	100%	25%
Copper	25%	–

Table 3.1: Performance of target materials relative to stainless steel

We also investigated the pump energy dependence for full target illumination for the gold-stainless steel target. Figure 3.4 shows that the gold target produced about twice the Xe^{2+} laser output energy as the stainless steel target over the full range of pump energies.

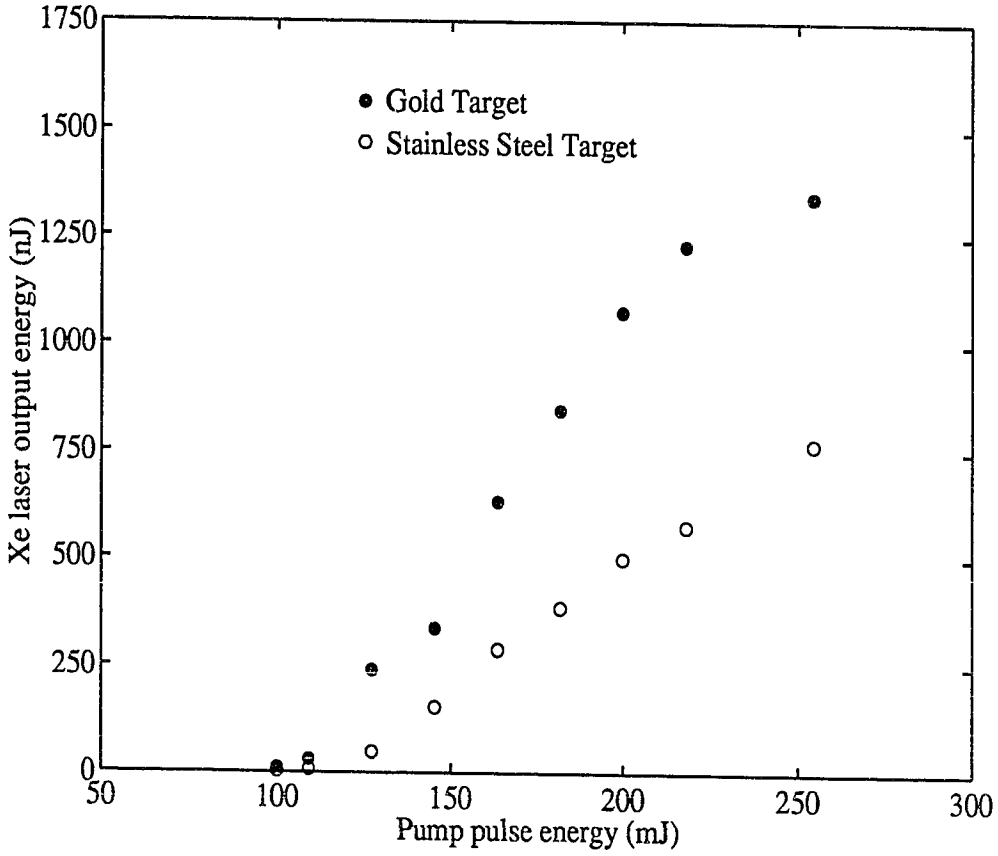

Figure 3.4: Xe laser output energy vs. pump energy for the gold-stainless steel target.

Standard deviations of less than $\pm 10\%$ were easily acheivable for each data point. The error range was largely dependent on the minimization of pump laser noise. The use of a digitizing storage oscilloscope during the experiments with cadmium and zinc targets made it easy to calculate standard deviations based on multiple data points. These deviations are presented on the cadmium and zinc gain curves of Figs. 3.3 and 3.4. We also observed minor variations between the different stainless steel targets. We attribute this variation to minor changes in pump beam focusing, in Xe pressure, and/or in the characteristics of the pump laser system occuring over the period required to change targets. During this time, the pump laser system displayed variations in pulse duration, beam profile, and pulse energy. Variation of these parameters was minimized by repeated adjustment of the pump system during the experiment. Furthermore, systematic changes in output over longer periods of time were the result of modifications and improvements in the pump laser system. For example, pump pulse durations of 200 psec were used for the gold-stainless steel target, while shorter, more powerful 100 psec pulses were subsequently used for all other targets. Thus, near-simultaneous comparison of sample materials to a standard surface is essential to get consistent results.

Consistency of output and target lifetime are also important criteria in selecting a target material. We have noticed that for new stainless steel targets, the first few pump pulses at a fixed location produce less 109 nm output energy than subsequent pulses. Apparently the initial pulses remove oxides or other residue that reduce plasma production efficiency, and we routinely expose a new target to a series of pump pulses before beginning measurements to insure consistency. We observed the same behaviour for both cadmium and zinc: several initial pump pulses at a fixed position were necessary to prepare the surface, while the next thirty or more shots in the same location showed little signal fluctuation. The gold plated target surface did not appear to require any initial "cleaning." In contrast, the copper plated target exhibited large pulse-to-pulse fluctuations in laser output, so large, in fact, that we were unable to make reliable measurements of the small signal gain coefficient. However, we were able to estimate a $\sim 25\%$ improvement in output for full pump beam illumination.

Surface ablation obviously limits the lifetime of plated targets; when the gold plated target was held stationary so that the pump repeatedly illuminated the same region, the 109 nm output signal was constant for about the first twenty pump pulses, after which the signal decreased to the stainless steel value as the plating was ablated. The thicker zinc and cadmium surfaces lasted more than twice as long. Our target

circumference consists of 1,600 75 μm wide strips, so a cadmium plated target should have a lifetime greater than 6.4×10^4 pulses, or about 3 hours at our pulse rate. Bulk, machined zinc or cadmium target rods are probably possible (most research budgets cannot accomodate solid gold target rods), but even solid stainless steel targets have a finite lifetime. Ablation removes the groove edges, and the rods must be remachined, perhaps every 50 hours for stainless steel. Target ablation also produces debris that ultimately deposits on chamber surfaces. The cadmium, gold, and zinc targets seemed to produce about equal amounts of debris, all somewhat more than from a stainless steel target. The copper target rapidly produced heavy debris contamination of the laser chamber. The mercury-wetted target of Yamakoshi, et al.[15], represents a clever method for avoiding ablation and debris problems while providing a high atomic number target surface.

The oxidation rate of a material following plating can be a significant consideration in target material selection, since we have seen how it influences output consistency. Both the zinc and cadmium targets showed visible oxidation after just a couple of hours in the atmosphere, with cadmium turning a dramatic sooty black. Thus, less than an hour after they were removed from the plating baths, the targets were mounted in the laser chamber and stored under vacuum. Initial pump pulses were still

necessary to remove the oxide layers and clean the surface residue. In contrast, the gold target was exposed to air for a number of days, requiring no special treatment other than a few initial pump pulses. Thus, while the output from a cadmium target may be slightly higher than that from a gold target, this advantage may be offset by the difficulties of minimizing the oxidation.

Chapter 4

Discussion

We have observed a $\sim$ 20% improvement in the gain coefficient and a $\sim$ 112% improvement in total energy for a Xe^{2+} 109 nm laser by plating the stainless steel target with cadmium. Significant improvements in output using zinc and gold were also observed. Use of these targets for the Xe^{2+} laser can reduce the pump energy required or reduce exposure times for applications such as imaging or photochemistry. With a copper target, the 109 nm laser output exhibited large pulse-to-pulse fluctuations, with the best values only slightly larger than those for the stainless steel target. The fluctuations appeared to result from the presence of surface oxides and a more rapid copper surface ablation. The rapid generation of copper debris, coupled with only a minor improvement in output energy, make copper targets a poor choice for the Xe^{2+} 109 nm laser.

It is reasonable to attribute the significant improvement in 109 nm laser output energy using a cadmium target to a higher pump to soft x-ray conversion efficiency, and/or to improved spectral properties. There are two plasma spectral factors that

could be important. Increased plasma emission at 100 eV, overlaping the Xe inner shell $4d$ photoionization cross section, would enhance the production of the upper laser level; in contrast, increased output of low energy photons could reduce gain by ionizing the upper laser level to Xe^{3+} (requiring about 7 eV), or by ionizing neutral Xe (12.1 eV) and producing extra electrons, which are believed to quench the Xe^{2+} gain [1]. Although several authors report spectra of laser-produced plasmas for different target materials [18, 19, 20, 21, 22], the experimental conditions were generally quite different from those used for the Xe^{2+} laser, and low photon energy spectra were not measured.

Table 4.1 summarizes the experimental conditions of the more relevant spectral studies, and highlights their differences compared to our study. Mochizuki, et al. [18], focused 532 nm, 1 nsec long pulses to a density of $10^{14}\,Wcm^{-2}$, nearly 1000 times higher than the density used here, onto a large number of target materials. Figure 13(a) in that paper shows that the conversion efficiency into the 100–200 eV band, the lowest energies measured, varies only moderately with atomic number for elements heavier than copper; certainly the efficiency of copper and gold appear identical under these conditions. Chaker, et al. [19], present experimental and theoretical conversion efficiencies as a function of atomic number using a 1064 nm, 500 psec long

Table 4.1: Summary of laser produced plasma spectral studies

Reference	Figure number	Intensity [Wcm^{-2}]	Pump wavelength [nm]	Pump pulse length [nsec]	Photon energy range [eV]
Mochizuki, et al. [18]	13(a)	$\sim 1 \times 10^{14}$	532	1	100–200
Chaker, et al. [19]	7(a)	$\sim 4 \times 10^{13}$	1064	0.5	100–750
Gerritsen, et al. [20]	8	$\sim 7 \times 10^{12}$	1064	15	250–800
Gerritsen, et al. [20]	6(a)	$\sim 7 \times 10^{12}$	1064	15	100–330
Kauffman, et al. [21]	3	$\sim 10^{11}$	532	7.5	92–100
Spitzer, et al. [22]	3, 4	$\sim 1 \times 10^{11}$	532	7.5	50-250, 80-150
Yamakoshi, et al. [15]	3	$\sim 3.5 \times 10^{10}$	1064	0.4	Xe^{2+} laser
This work	–	$\sim 10^{11}$	1064	0.1–0.2	Xe^{2+} laser

pump pulse focused to a density of $4 \times 10^{13}\,\mathrm{Wcm^{-2}}$. Their theoretical curve for conversion into the 100–750 eV band shows a periodic dependence with variations of about a factor of three. Their measurements of copper and gold targets match the theory, with gold yielding 2.5-times the efficiency of copper. They did not measure a cadmium target, but it would fall at a minimum of their calculated curve, with an efficiency about equal to copper, in contrast to our results. Gerritsen, et al. [20], present experimental data from 15 target materials using a 532 nm, 15 nsec long pump focused to $7 \times 10^{12}\,\mathrm{Wcm^{-2}}$. The conversion efficiency into the 250–800 eV band shows peaks corresponding to atomic shells. The peaks, however, are shifted from the theory of Chaker, et al., with maxima near titanium (atomic number Z=22), cadmium (Z=48), and gold (Z=79). The yield for gold was also about twice that of copper, while the maxima at cadmium was about 25% above that of gold. This is more consistent with our observations, except this data also indicates that an iron or nickel target (the main components of stainless steel) would have a yield slightly better than a copper target.

Perhaps more relevant are the detailed emission spectra (resolution ~ 7 eV) from 100 to 330 eV shown in Fig. 6 of Gerritsen, et al. Iron and copper show about equal yields at 100 eV, while gold is 30% higher. Cadmium was not measured, but it is

spanned in atomic number by silver (Z=47), having a yield 40% higher than iron, and by tin (Z=50) with a yield about equal to iron. From these curves, the best target materials for the Xe^{2+} laser appear to be tantalum (Z=73) and lead (Z=82), both with yields at 100 eV over twice as high as iron and 50% greater than gold. Tantalum is very difficult to machine and to electroplate. We tried several stainless steel target rods that were "flame-sprayed" or plasma deposited with tantalum [23]. These coatings are very granular; thick coatings filled in the grooves and thin coatings were irregular. We were unable to observe any 109 nm output using these targets. While the efficiency of a lead plated target might be high, we suspect that the output consistency and debris problems would be very similiar to those of copper.

The most pertinent work in terms of experimental conditions would appear to be that of Kauffman, et al [21]. They performed a Z-scaling study for 16 materials, recording X-ray conversion efficiency into a narrow ~ 8 eV band centered at 96.5 eV. While the pump excitation wavelength was shorter (532 nm) and the pulse duration was longer (7.5 nsec) than in our studies, the intensity on target was comparable at $\sim 10^{11}\,\mathrm{Wcm^{-2}}$. Their results also show peaks corresponding to atomic shells, but shifted from those of Chaker, et al., and Gerritsen, et al. The yield for gold was nearly twice that of copper, and the cadmium yield fell between copper and gold.

Again, iron and nickel targets had a yield equal to or better than copper. The results of Gerritsen, et al., and Kauffman, et al., are very similar despite recording different energy ranges. Thus, even under the most similar experimental conditions, their measurements do not fully explain our observations, perhaps indicating the importance of the low photon energy spectra of different targets.

The studies cited above and our own work indicate that target materials of high atomic number are likely to be more efficient for pumping the Xe laser. Yet, it is simplistic to think that target atomic number is the only important parameter, or even an independent parameter. This is shown clearly in the work of Spitzer, et al. [22], who made detailed spectral measurements of laser-produced plasma efficiency in the range of 50–250 eV for gold and tin targets. Both gold and tin have (at least local) emission peaks near 100 eV that match the Xe inner shell photoionization, so it is not surprising that we found gold to be a good target material. However, the pump conversion efficiency into the 80–150 eV band varies significantly with focal spot size and power density, and *the dependence is different for the two materials.* For example, the conversion efficiency for tin maximizes at a value of focal power density which depends on spot size. In contrast, the efficiency of a gold target shows no maximum in the range studied, but increases steadily with power density for all

spot sizes. Similarly, Yamakoshi, et al. [15], found that the Xe^{2+} laser gain coefficient using a mercury target was higher than that for gold at a pump power intensity of $1 \times 10^{10}\,\mathrm{Wcm^{-2}}$, while the situation was reversed at $3.5 \times 10^{10}\,\mathrm{Wcm^{-2}}$.

Chapter 5

Conclusions and Future Directions

Our work has shown that a simple change of target material can result in significant improvements in the Xe^{2+} 109 nm laser performance. Use of a cadmium plated target provided a $\sim$ 20% improvement in small signal gain and a $\sim$ 112% improvement in output over a stainless steel target. A linear dependence of Xe laser output on pump energy was also observed for the plated targets. Thus, we can expect only as much as a linear improvement in laser performance using a larger pump system. Considering the frailty and complexity of the pump system, a change of target material is clearly the preferred option. The best performing targets in this experiment generated acceptable amounts of debris, each only a bit more than stainless steel.

Other promising target materials remain to be tested in future experiments. We would like to make another attempt at a tantulum target, a material which appears to be as good or better than gold and cadmium in most of the literature. It would also be useful to confirm that the performance of a tin target is comparable to a gold or cadmium target, since tin is cheaper than gold and oxidizes slower than cadmium.

Despite these useful results, it is clear that we have explored only part of the full parameter space of target conditions, and our ranking of materials would probably change for different conditions of pump wavelength, pulse length, power density, and focal geometry. Our results represent a good starting point for a detailed optimization of pumping conditions in other situations.

Bibliography

[1] H. C. Kapteyn and R. W. Falcone, "Observation of a short-wavelength laser pumped by Auger decay," *Physical Review Letters*, vol. 57, pp. 2939–2942, 1986.

[2] D. J. Walker, C. P. J. Barty, G. Y. Yin, J. F. Young, and S. E. Harris, "Observation of super Coster–Kronig pumped gain in Zn III," *Optics Letters*, vol. 12, pp. 894–896, 1987.

[3] H. C. Kapteyn and R. W. Falcone, "Auger-pumped short-wavelength lasers in xenon and krypton," *Physical Review A*, vol. 37, pp. 2033–2038, 1988.

[4] S. J. Benerofe, G. Y. Yin, C. P. J. Barty, J. F. Young, and S. E. Harris, "116 nm H_2 laser pumped by a traveling-wave photoionization electron source," *Physical Review Letters*, vol. 66, pp. 3136–3139, 1991.

[5] C. P. J. Barty, G. Y. Yin, J. E. Field, D. A. King, K. H. Hahn, J. F. Young, and S. E. Harris, "Studies of a 96.9 nm laser in neutral cesium," *Physical Review A*, vol. 46, pp. 4286–4296, 1992.

[6] C. Tóth, J. F. Young, and R. Sauerbrey, "Optical gain in the ionic excimer $Cs^{2+}F^{-}$ excited by soft x-rays from a laser-produced plasma," *Optics Letters*, vol. 18, pp. 2120–2122, 1993.

[7] D. M. P. Holland, K. Codling, J. B. West, and G. V. Marr, "Multiple photoionisation in the rare gases from threshold to 280eV," *Journal of Physics B: Atomic and Molecular Physics*, vol. 12, no. 15, pp. 2465–2484, 1979.

[8] C. E. Max, "Physics of the coronal plasma in laser fusion targets," in *Laser–Plasma Interaction* (R. Balian and C. C. Adam, eds.), pp. 302–410, North-Holland Publishing, 1982.

[9] W. L. Kruer, *The Physics of Laser Plasma Interactions.* Addison-Wesley, 1988.

[10] R. M. More, "Atomic physics of laser-produced plasmas," in *Physics of Laser Plasma* (A. Rubenchik and S. Witkowski, eds.), Handbook of Plasma Physics. Volume 3, ch. 2, pp. 63–110, North-Holland, 1991.

[11] G. Y. Yin *et al.*, "Low-energy pumping of a 108.9 nm xenon Auger laser," *Optics Letters*, vol. 12, pp. 331–333, 1987.

[12] M. H. Sher, J. J. Macklin, J. F. Young, and S. E. Harris, "Saturation of the Xe III 109 nm laser using traveling-wave laser-produced-plasma excitation," *Optics Letters*, vol. 12, pp. 891–893, 1987.

[13] M. H. Sher, S. J. Benerofe, J. F. Young, and S. E. Harris, "2-Hz 109 nm mirrorless laser," *Journal of the Optical Society of America B*, vol. 8, pp. 114–116, 1991.

[14] T. S. Clement, C. Tóth, J. Wu, and J. F. Young, "A reasonably practical XUV laser for applications," *IEEE Journal of Quantum Electronics*, vol. 30, pp. 2136–2140, 1994.

[15] H. Yamakoshi, C. T. Chin, S. Jaimungal, P. R. Herman, F. Budnik, G. Kulesár, L. Zhao, and R. S. Majoribanks, "Extreme-ultraviolet laser photo-pumped by a self-healing Hg target," in *Applications of Laser Plasma Radiation*, vol. 2015, (Bellingham, WA 98227-0010), SPIE, 1993.

[16] C. Tóth, "Simple optical pulse lengthening setup for the subnanosecond range," *Optics and Photonics News/Engineering and Laboratory Notes*, vol. 8, 1995. (in press).

[17] J. T. Hunt, J. A. Glaze, W. W. Simmons, and P. A. Renard, "Suppression of self-focusing through low-pass spatial filtering and relay imaging," *Applied Optics*, vol. 17, no. 13, pp. 2053–2057, 1978.

[18] T. Mochizuki, T. Yabe, K. Okada, M. Hamada, N. Ikeda, S. Kiyokawa, and C. Yamanaka, "Atomic-number dependence of soft x-ray emission from various targets irradiated by a 0.53 μm wavelength laser," *Physical Review A*, vol. 33, pp. 525–539, 1986.

[19] M. Chaker, H. Pépin, V. Bareau, and B. Lafontaine, "Laser plasma x-ray sources for microlithography," *Journal of Applied Physics*, vol. 63, pp. 892–899, 1988.

[20] H. C. Gerritsen, H. van Brug, F. Bijkerk, and M. J. van der Wiel, "Laser-generated plasma as soft x-ray source," *Journal of Applied Physics*, vol. 59, pp. 2337–2344, 1986.

[21] R. L. Kauffman, D. W. Phillion, and R. C. Spitzer, "X-ray production $\sim 13\,\mathrm{nm}$ from laser-produced plasmas for projection x-ray lithography applications," *Applied Optics*, vol. 32, no. 34, pp. 6897–6900, 1993.

[22] R. C. Spitzer, R. L. Kauffman, T. Orzechowski, D. W. Phillion, and C. Cerjan, "Soft x-ray production from laser produced plasmas for lithography applications," *Journal of Vacuum Science and Technology B*, vol. 11, no. 6, pp. 2986–2989, 1993.

[23] Flame Spray Coating Co., Inc. 33847 Doreka, Fraser, MI 48026.